

Optimisation of In Vitro Fertilisation

A special topic for Mathematical Modelling and Scientific Computing in Mathematical Physiology

George Hildick-Smith

February 21, 2026

© 2026 George Hildick-Smith. This work is licensed under CC BY-NC-ND 4.0, https://creativecommons.org/licenses/by-nc-nd/4.0/. Third party images and quotations remain the property of their owners.

1 Introduction

In 1959, pioneering work by Min Chueh Chang established the feasibility of artificial mammalian fertilisation [1]. Subsequently, the birth of Louise Brown in the UK in 1978 marked the first successful application of in vitro fertilization (IVF) in humans. Since then, extensive research and legislative efforts have aimed to mitigate the risks associated with IVF for both women and children involved. However, the procedure continues to present diverse challenges in both physical and psychological areas [2].

Another important aspect of IVF is the physical risk associated with multiple pregnancies. These occur more frequently with IVF than with natural reproduction because multiple embryos are implanted to increase pregnancy success rates. This can cause miscarriage, high blood pressure, and gestational diabetes for the mother. For the child, the risks include a premature and low-weight birth which can have many complications [3] [4]. Because of these severe risks, the Human Fertilisation and Embryology Authority (HFEA) suggests that at most two embryos are transferred to a womb if the woman is under 40 years old and three if over [4]. Balancing the likelihood of pregnancy with the risks of multiple births and associated problems adds complexity to determining the optimal number of embryos. In light of these challenges, controlled ovarian stimulation (COS) is critical to the success of IVF, and mathematical modelling offers valuable tools for informing the embryologist's decisions. In this work, we examine how modelling and optimisation methods can be applied to improve results in IVF, focusing on strategies to maximise oocyte[1] yield from the ovaries, as seen in the ultrasound in Figure 1. At the same time, it is essential to consider other risks such as ovarian hyperstimulation syndrome (OHSS) [3].

The financial costs of IVF are also significant. In the UK, a single cycle of IVF can cost between £3,000 and £5,000 [5]. Therefore, optimising treatment protocols not only improves health outcomes but also reduces financial burdens on patients. With this in mind, we will look to reduce costs in terms of the amount of medication supplied to the patient during the COS phase of IVF.

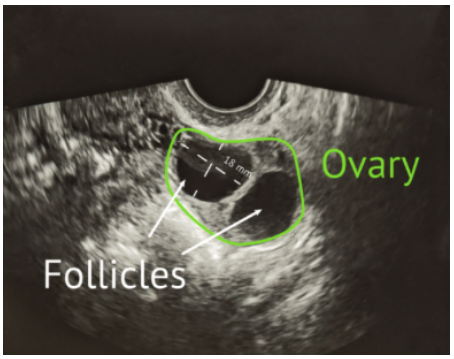


Figure 1: Ultrasound image of ovarian follicles, adapted from [6].

[1] An *oocyte* is an immature egg cell that develops within the ovarian follicles at the beginning of the menstrual cycle.

2 How IVF Works

To understand the dynamics involved in IVF, we first need to understand the process itself. It is a process in which an egg is fertilised by sperm outside the body, in vitro and then at least one fertilised egg (an embryo) is implanted in the uterus in the hope of achieving a successful pregnancy. IVF is typically used when couples face infertility issues or require a sperm donor. There are roughly four stages to IVF treatment.

1. **Medication to produce multiple eggs:** The goal here is to stimulate the ovaries to produce multiple mature eggs. By retrieving multiple eggs, the embryologist then has options when selecting the egg, which can enhance the overall success rates of IVF. In normal menstrual cycles, typically only one egg matures and is released. For more information on this, see Appendix C. In IVF, medication such as follicle stimulating hormone (FSH) is administered to the patient to encourage the development of multiple follicles in the ovaries. The levels of luteinizing hormone (LH) in the blood must be monitored closely such that premature ovulation does not occur. This is the stage we will focus on modelling in this report as it is critical to the success of IVF.
2. **Egg retrieval:** Once the eggs have matured, they are collected from the ovaries using a minor surgical procedure called transvaginal ultrasound aspiration. This is usually done under sedation to minimise discomfort.
3. **Fertilisation and embryo culture:** The eggs are then fertilised with sperm. This is done through either 'conventional' insemination, where eggs and sperm are mixed together in a Petri dish, or through intracytoplasmic sperm injection (ICSI), where a single sperm is injected directly into an egg with a syringe. The fertilised eggs are kept for several days, allowing them to grow.
4. **Embryo transfer:** Finally, one or more healthy embryos are selected and transferred into the uterus. The number of embryos transferred is critical and balances the chances of pregnancy against the risks of multiple births.

When medication is prescribed, it is usually a 'long' or 'short' protocol. In a long protocol, the patient receives gonadotropin-releasing hormone (GnRH) agonists to suppress their natural hormone production before starting FSH. This helps prevent premature ovulation. In a short protocol, during the FSH stimulation phase, GnRH antagonists are also used to quickly suppress LH surges, allowing a shorter duration of treatment. To simplify our model, we will focus on the 'short' protocol, which reduces the number of variables and simplifies the dynamics.

3 Derivation of Mathematical Model

To obtain a feasible working approximation of the processes involved in IVF, we will make a few assumptions about both the patient and the model. These assumptions are not exhaustive, nor are they necessarily true in all cases; however, they give an accurate representation of the behaviours we are interested in.

3.1 Assumed Properties of the Patient

1. The patient has a menstrual cycle of 28 days, hence ovulation occurs on day 14.
2. The patient responds normally to FSH stimulation.
3. There are no underlying health conditions affecting hormone levels.
4. Environmental and lifestyle factors are constant and do not affect the cycle.

3.2 Assumed Properties of the Model

1. The model focuses only on hormonal dynamics and follicle development.
2. The effects of medications are considered instantaneous.
3. The model does not account for stochastic variations in hormone levels.
4. The model ignores any spatial dynamics within the body.

3.3 Model Development

To develop our mathematical model, we first identify the key hormones and processes involved in IVF up to egg retrieval. The primary hormones of interest are FSH, LH, and estradiol (E2). The components of the model are: u the dose of FSH injected over time; F, L, E, the concentrations of FSH, LH, and E2 in the bloodstream, respectively; M the number of mature follicles; α the rate of follicle maturation. Note that u and α are inputs to the system, while the rest are variables. In the subsections on the next page, we justify each of the relationships shown in Figure 2 where green arrows represent production / stimulation / administration and red represents inhibition.

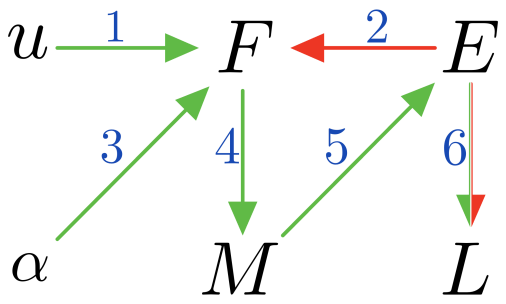


Figure 2: Diagram of relationships for the proposed model.

3.3.1 Justification of 1

Administration of FSH is usually performed through injections at specific times during the treatment cycle. This external input can be modelled as a time-dependent function $u(t)$ which is a piecewise continuous function representing the dose of FSH administered at time t. This function can take various forms depending on the treatment protocol, such as constant, periodic, or more complex dosing schedules.

3.3.2 Justification of 2 and 6

Studying the dynamics described in Section 2.2.2 of [7] and the results section of [8], we see that E2 inhibits the production of FSH when E2 is high enough, giving relationship 2. Then, E2 can promote the rapid production of LH if there is a sustained high level; the green side of relationship 2. Alternatively, low levels of E2 inhibit LH, hence the red side of relationship 2.

3.3.3 Justification of 3 and 4

There is a constant baseline rate of FSH production that occurs naturally in the body; this corresponds to relationship 3 and is independent of $u(t)$. The FSH in the bloodstream will eventually find its way to the ovaries where it binds to receptors on the surface of the follicles [9]. This binding stimulates the follicles to grow and mature, hence relationship 4.

3.3.4 Justification of 5

When follicles mature, they produce E2 via theca[2] and granulosa cells[3]. Theca cells produce androgens that are then converted to E2 by granulosa cells [9]. However, to simplify our model, we will assume that the production of E2 is directly related to the number of mature follicles.

3.3.5 Decay Terms

Finally, although not explicitly shown in the diagram, we need to account for the natural clearance of hormones from the bloodstream and decay of follicles. Selgrade and Harris justify that this can be modelled as a first-order decay process [10]. This assumption simplifies the dynamics and combines effects such as metabolic breakdown, renal clearance, cellular uptake and chemical instability or atresia[4] for follicles into a single term in each equation.

[2] *Theca cells* form the outer layer of the follicle and produce androgens from cholesterol.

[3] *Granulosa cells* form the inner layer surrounding the oocyte; they respond primarily to FSH and express the enzyme aromatase, which converts androgens into estradiol.

[4] *Atresia* is the process of follicle degeneration and resorption in the ovary.

3.4 The Nature of Hormone Interactions

Looking at the work done by Selgrade and Harris, they develop a model of the synthesis, release, and clearance of LH through the menstrual cycle [10]. In doing so, they look at both the LH in the bloodstream and in what they call the reserve pool. A copy of their full system for LH can be seen in Appendix D. However, we are only interested in the hormones currently in the bloodstream, but we note the particular system they use to model LH synthesis as

$$syn_{LH}(E_2, P_4) = \frac{V_{0,LH} + \frac{V_1, LH E_2(t-d_E)^8}{(Km_{LH})^8 + E_2(t-d_E)^8}}{1 + \frac{P_4(t-d_P)}{Ki_{LH,P}}}. \tag{1}$$

The important part to note here is the (scaled) Hill function in the numerator, which models the positive feedback of E2 on LH synthesis. This is a common way to model how hormones both promote and inhibit each other and can be thought of as a biological switch. We will use similar functions in our model. In general, a Hill function has the form,

$$H(x) = \frac{x^n}{K^n + x^n}, \tag{2}$$

where K is the half-saturation constant and n is the Hill coefficient determining the steepness of the curve. This function captures the threshold-like activation and saturation behaviour as shown in Figure 3. This means that when x approaches K, we start to activate a response, e.g., the inhibition of FSH by E2.

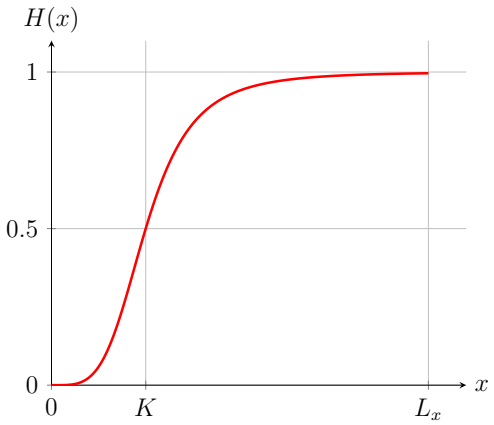


Figure 3: Example of a Hill function with $n = 4$ and $K = 20$.

We will use this function form to model the interactions between E2 and FSH, and E2 and LH in our proposed model. It will also be used to simulate the natural production of FSH.

3.5 The Mathematical Model

Given the justifications above, we now present our new proposed mathematical model for the hormonal dynamics during IVF treatment up to egg retrieval as

$$F_\tau = -\gamma_F F - \beta_F F H_2(E) + \alpha\big(1 - H_3(F)\big) + u, \tag{3a}$$

$$E_\tau = -\gamma_E E + \beta_E M, \tag{3b}$$

$$L_\tau = -\gamma_L L + \beta_{L^+} H_6^+(E) - \beta_{L^-} L\big(1 - H_6^-(E)\big), \tag{3c}$$

$$M_\tau = -\gamma_M M + \beta_M F. \tag{3d}$$

Here, we have that

- F, E, L are the concentrations of FSH, E2, and LH in the bloodstream and note only the τ subscript denotes differentiation with respect to time τ (i.e. $\frac{\partial}{\partial \tau}$),
- M is the number of mature follicles,
- γ_F, γ_E, γ_L, γ_M are the clearance/decay rates of FSH, E2, LH, and mature follicles respectively,
- β_F, β_E, β_{L^+}, β_{L^-}, β_M are the production rates of FSH, E2, LH (positive and negative feedback), and mature follicles, respectively,
- all Hill functions are of the form $H_i(x) = \frac{x^{n_i}}{K_i{}^{n_i} + x^{n_i}}$ where K_i and n_i are parameters to be determined and i denotes the relationship in Figure 2, specifically:
  - $H_2(E)$ models the inhibition of FSH production by E2,
  - $H_3(F)$ models the natural production of FSH,
  - $H_6^+(E)$ models the positive feedback of E2 on LH production,
  - $H_6^-(E)$ models the negative feedback of E2 on LH production.
- $u(\tau)$ is the dosage of FSH injected over time,
- α is the rate of natural follicle maturation.

We note that in Equation (3c) for LH we have two separate Hill functions, $H_6^+(E)$ and $H_6^-(E)$. This is to capture both the positive and negative feedback effects of E2 on LH production depending on the value of E2. The values of n will need to be high as this will elicit a decisive response as to which behaviour is occurring, and for simplicity, they can be the same ($n_6 = n_6^+ = n_6^-$). However, the half-saturation constants K will be different to capture the different thresholds for positive and negative feedback.

3.6 Non-dimensionalisation of the Model

To reduce the number of parameters in the model and simplify the analysis, we will non-dimensionalise the system. The full details of this process can be found in Appendix E. If we let

$$\tau = \frac{1}{\gamma_F}\, t, \quad F = \frac{\alpha}{\gamma_F}\, f, \quad E = \frac{\alpha\beta_E\beta_M}{\gamma_F^3}\, e, \quad L = \frac{\beta_{L^+}}{\gamma_F}\, \ell, \quad M = \frac{\alpha\beta_M}{\gamma_F^2}\, m,$$

and write the Hill functions out fully, we obtain the non-dimensional system

$$\frac{\mathrm{d}f}{\mathrm{d}t} = -f - \lambda_F \frac{f e^{n_2}}{\kappa_2^{n_2} + e^{n_2}} + \left(1 - \frac{f^{n_3}}{\kappa_3^{n_3} + f^{n_3}}\right) + \phi(t), \tag{4a}$$

$$\frac{\mathrm{d}e}{\mathrm{d}t} = -\delta_E e + m, \tag{4b}$$

$$\frac{\mathrm{d}\ell}{\mathrm{d}t} = -\delta_L \ell + \frac{e^{n_6}}{\left(\kappa_6^+\right)^{n_6} + e^{n_6}} + \lambda_{L^-} \frac{\ell e^{n_6}}{\left(\kappa_6^-\right)^{n_6} + e^{n_6}}, \tag{4c}$$

$$\frac{\mathrm{d}m}{\mathrm{d}t} = -\delta_M m + f. \tag{4d}$$

Here, we have that

- $\delta_E = \frac{\gamma_E}{\gamma_F}$, $\delta_L = \frac{\gamma_L + \beta_{L^-}}{\gamma_F}$, $\delta_M = \frac{\gamma_M}{\gamma_F}$ are the dimensionless clearance/decay rates,
- $\kappa_2 = \frac{K_2\gamma_F^3}{\alpha\beta_E\beta_M}$, $\kappa_3 = \frac{K_3\gamma_F}{\alpha}$, $\kappa_6^+ = \frac{K_6^+\gamma_F^3}{\alpha\beta_E\beta_M}$, $\kappa_6^- = \frac{K_6^-\gamma_F^3}{\alpha\beta_E\beta_M}$ are the dimensionless half-saturation constants,
- $\lambda_F = \frac{\beta_F}{\gamma_F}$, $\lambda_{L^-} = \frac{\beta_{L^-}}{\gamma_F}$ are dimensionless production rate parameters,
- $\phi(t) = \frac{1}{\alpha} u\left(\frac{t}{\gamma_F}\right)$ is the dimensionless FSH dosage.

We note that the second term in $\frac{\mathrm{d}f}{\mathrm{d}t}$ models the inhibition of FSH production by E2, and hence κ_2 should be high to mimic this behaviour. Similarly, the third term models the natural production of FSH; this should only stop when the body detects there is already a lot of FSH in the bloodstream, hence κ_3 should also be high.

For $\frac{\mathrm{d}\ell}{\mathrm{d}t}$, the Hill functions here model the positive and negative feedback of E2 on LH production respectively. The positive feedback should occur only when E2 is high enough, hence κ_6^+ should be high. However, the negative feedback should occur when E2 is low, hence κ_6^- should also be low. It is also worth noting that δ_L includes both the natural clearance of LH and the negative feedback production rate term β_{L^-}, so it will be larger than the other δ values. We should also have that $\delta_L > \lambda_{L^-}$ from its derivation.

4 Analytical Analysis of the Model

4.1 Feasibility of the Model

It is worth checking that the model gives biologically feasible results. That is, all variables should remain non-negative for non-negative initial conditions and dosage $\phi(t) \geq 0$. We check this by evaluating each ordinary differential equation (ODE) when that specific variable is zero. If the derivative is non-negative, then the variable cannot become infeasible. Taking each ODE in turn gives:

- Equation (4a): if $f = 0$, then $\frac{\mathrm{d}f}{\mathrm{d}t} = 1 + \phi(t) \geq 0$;
- Equation (4d): if $m = 0$ and since $f \geq 0$, then $\frac{\mathrm{d}m}{\mathrm{d}t} = f \geq 0$;
- Equation (4b): if $e = 0$ and since $m \geq 0$, then $\frac{\mathrm{d}e}{\mathrm{d}t} = m \geq 0$;
- Equation (4c): if $\ell = 0$ and since $e \geq 0$, then $\frac{\mathrm{d}\ell}{\mathrm{d}t} = \frac{e^{n_6}}{(\kappa_6^+)^{n_6} + e^{n_6}} \geq 0$.

In the formation of the model, to ensure feasibility, we multiplied the negative terms (excluding decay / atresia terms) in Equations (4a) and (4d) by the respective variable.

4.2 Equilibria of the Model

We start by setting the time derivatives in Equations (4a) to (4d) and of ϕ to zero, so

$$0 = -f^* - \lambda_F \frac{f^*(e^*)^{n_2}}{\kappa_2^{n_2} + (e^*)^{n_2}} + \left(1 - \frac{(f^*)^{n_3}}{\kappa_3^{n_3} + (f^*)^{n_3}}\right) + \phi, \tag{5a}$$

$$0 = -\delta_E e^* + m^*, \tag{5b}$$

$$0 = -\delta_L \ell^* + \frac{(e^*)^{n_6}}{(\kappa_6^+)^{n_6} + (e^*)^{n_6}} + \lambda_{L^-} \frac{\ell^*(e^*)^{n_6}}{(\kappa_6^-)^{n_6} + (e^*)^{n_6}}, \tag{5c}$$

$$0 = -\delta_M m^* + f^*. \tag{5d}$$

From Equations (5b) and (5d), we find m^* and f^* in terms of e^*, giving

$$m^* = \delta_E e^*, \tag{6}$$

$$f^* = \delta_M m^* = \delta_M \delta_E e^*. \tag{7}$$

Rearranging Equation (5c) for ℓ_* we arrive at

$$\ell^* = \left[\frac{(e^*)^{n_6}}{(\kappa_6^+)^{n_6} + (e^*)^{n_6}}\right] \Big/ \left[\delta_L - \lambda_{L^-} \frac{(e^*)^{n_6}}{(\kappa_6^-)^{n_6} + (e^*)^{n_6}}\right]. \tag{8}$$

Substituting Equation (7) into Equation (5a) gives a condition for ϕ in terms of e^*,

$$\phi(e^*) = \delta_M \delta_E e^* + \lambda_F \frac{\delta_M \delta_E (e^*)^{n_2+1}}{\kappa_2^{n_2} + (e^*)^{n_2}} - \left(1 - \frac{(\delta_M \delta_E e^*)^{n_3}}{\kappa_3^{n_3} + (\delta_M \delta_E e^*)^{n_3}}\right). \tag{9}$$

4.3 Feasibility of Equilibria

We need to check if all of these equilibria and dosages, ϕ, are feasible. That is, all variables and ϕ must be non-negative. From Equations (6) and (7), we see that as long as e^* is non-negative, both m^* and f^* will also be non-negative. However, for ℓ^* to be non-negative, we need the denominator in Equation (8) to be positive, i.e.

$$0 < \delta_L - \lambda_{L^-} \frac{(e^*)^{n_6}}{(\kappa_6^-)^{n_6} + (e^*)^{n_6}}. \tag{10}$$

This is always true if $\delta_L > \lambda_{L^-}$; this was noted in the derivation of δ_L. We also need to ensure that $\phi \geq 0$. Multiplying through Equation (9) by the denominators gives

$$\begin{aligned} 0 \leq & (\delta_M \delta_E e^* - 1)(\kappa_2^{n_2} + (e^*)^{n_2})(\kappa_3^{n_3} + (\delta_M \delta_E e^*)^{n_3}) \\ & + (\lambda_F \delta_M \delta_E (e^*)^{n_2+1})(\kappa_3^{n_3} + (\delta_M \delta_E e^*)^{n_3}) \\ & + (\delta_M \delta_E e^*)^{n_3}(\kappa_2^{n_2} + (e^*)^{n_2}). \end{aligned} \tag{11}$$

This is a polynomial in e^* of degree $n_2 + n_3 + 1$, and hence in general is not analytically solvable for e^* when set to zero. However, it can easily be shown that $\phi(e^*)$ has a single positive root that we shall call $e_{\min}$. Using Equation (9), $\phi(0) = -1$ and $\lim_{e^* \to \infty} \phi(e^*) = \infty$. Then consider the derivative of $\phi(e^*)$,

$$\frac{d\phi}{de^*} = \delta_M \delta_E + \lambda_F \delta_M \delta_E \frac{(n_2+1)\kappa_2^{n_2}(e^*)^{n_2} + (e^*)^{2n_2}}{(\kappa_2^{n_2} + (e^*)^{n_2})^2} + \frac{n_3(\delta_M \delta_E)^{n_3}\kappa_3^{n_3}(e^*)^{n_3-1}}{(\kappa_3^{n_3} + (\delta_M \delta_E e^*)^{n_3})^2}. \tag{12}$$

Equation (12) is positive for all $e^* \geq 0$, hence ϕ is strictly monotonically increasing with respect to e^*. Therefore, by the intermediate value theorem, there exists a single positive root for which $\phi = 0$ and for all e^* greater than this, ϕ will be positive. Because this root is positive, for all feasible ϕ, the corresponding e^* (and hence all other equilibria by Equations (6) to (8)) will also be feasible. So in practical senses, the model works. What this also shows is there is a small interval of e^* that would require a negative dosage of FSH to achieve, which is not possible biologically[5]. This is illustrated in Figure 4 by the values of e^* less than $e_{\min}$. Analogously, because we have expressed the equilibria of f, ℓ and m in terms of e^*, there are also equilibria values which are also biologically infeasible.

[5]For the e^* such that ϕ is negative, this is essentially asking us to remove FSH from the bloodstream, which may be possible through dialysis, and could be useful for a patient producing too much FSH naturally. However, there are other methods to reduce FSH levels, such as using GnRH agonists or antagonists, which suppress the natural production of FSH by the pituitary gland [11]. As this is not the focus of this work or the point of the model, we will not explore $\phi < 0$ further.

We note that if $\delta_M \delta_E e^* \geq 1$, then the first term in Equation (11) is non-negative. The other two terms are always non-negative, hence a sufficient condition for $\phi \geq 0$ is

$$e^* \geq \frac{1}{\delta_M \delta_E}. \tag{13}$$

Hence, for all e^* that satisfy this condition, there exists a feasible (positive) constant dose, ϕ, that results in feasible equilibria for all variables. In practice, we control ϕ directly through FSH injections, not e^*. Hence, if we evaluate Equation (9) using $e_g = \frac{1}{\delta_M \delta_E}$, then we obtain the corresponding constant dose of FSH,

$$\phi_g = \frac{\lambda_F}{(\kappa_2 \delta_M \delta_E)^{n_2} + 1} + \frac{1}{\kappa_3^{n_3} + 1}. \tag{14}$$

Simply put, ϕ_g is a guaranteed feasible dose of FSH that will result in all variables converging to analytical feasible equilibria. Both ϕ_g and e_g can be seen in Figure 4.

We may want to find $e_{\min}$ as plotted in Figure 4 (purple dashed line). Computationally, we have two immediate ways we can find $e_{\min}$. One is to simulate the system with $\phi = 0$ and see what e^* the system converges to. Another (better method) would be to use the Newton-Raphson method, as we have ϕ and ϕ' analytically. This would be much faster than simulating the system as we would only need to evaluate Equations (9) and (12) a few times to converge to $e_{\min}$.

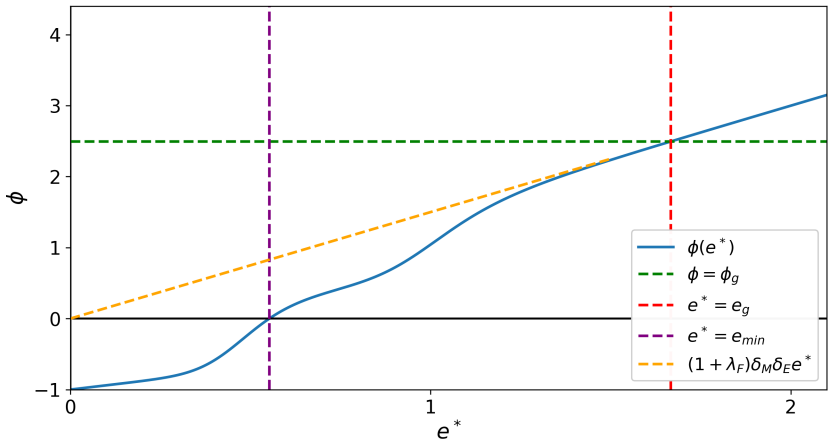


Figure 4: Plot showing the equilibrium for e^* against dosage ϕ. An interactive version of this plot is available at https://www.desmos.com/calculator/xo7dov3xie. The parameters were chosen to show the observable properties (listed in Appendix B).

Finally, we also show the limiting behaviour of ϕ as e^* becomes large (yellow dashed line). From Equation (9), as $e^* \to \infty$, the Hill functions tend to 1, which gives us the approximation,

$$\phi(e^*) \approx (1 + \lambda_F)\delta_M \delta_E e^*. \tag{15}$$

Now consider things from the practical perspective where e^* is a function of ϕ. This is the more natural way to perceive this problem as we can in practice control ϕ, not e^*. Despite the fact that we are unable to invert Equation (9) into a closed form expression, because the derivative is strictly monotonically increasing, we say that there exists a unique inverse function $e^*(\phi)$. However, we can invert the approximation Equation (15) as

$$e^*(\phi) \approx \frac{1}{(1+\lambda_F)\,\delta_M\delta_E}\phi. \tag{16}$$

Analogously, as f^* and m^* are linear functions of e^*, they will also behave approximately linearly with respect to large ϕ. Specifically, from Equations (6) and (7) and the above approximation, we have

$$f^*(\phi) \approx \frac{\delta_M\delta_E}{(1+\lambda_F)\,\delta_M\delta_E}\phi = \frac{1}{1+\lambda_F}\phi, \tag{17}$$

$$m^*(\phi) \approx \frac{\delta_E}{(1+\lambda_F)\,\delta_M\delta_E}\phi = \frac{1}{(1+\lambda_F)\,\delta_M}\phi. \tag{18}$$

However, for LH, we see from Equation (8) that as $e^* \to \infty$ (assuming still that this is due to $\phi \to \infty$), ℓ^* can be approximated as

$$\ell^*(\phi) \approx \left[\frac{1}{(\omega^+/\phi)^{n_6}+1}\right] \Big/ \left[\delta_L - \frac{\lambda_{L^-}}{(\omega^-/\phi)^{n_6}+1}\right], \tag{19}$$

where $\omega^{\pm} = \kappa_6^{\pm}\,(1+\lambda_F)\,\delta_M\delta_E$. As ϕ grows, this approaches a horizontal asymptote. Both of $(\omega^{\pm}/\phi)$ tend to zero, and we are left with $\ell_{\max} = \lim_{\phi\to\infty}\ell^* = \frac{1}{\delta_L-\lambda_{L^-}}$. We compare these approximations to numerical solutions of the system (Equations (5b) to (5d)) for large ϕ values to verify their accuracy in Figure 5.

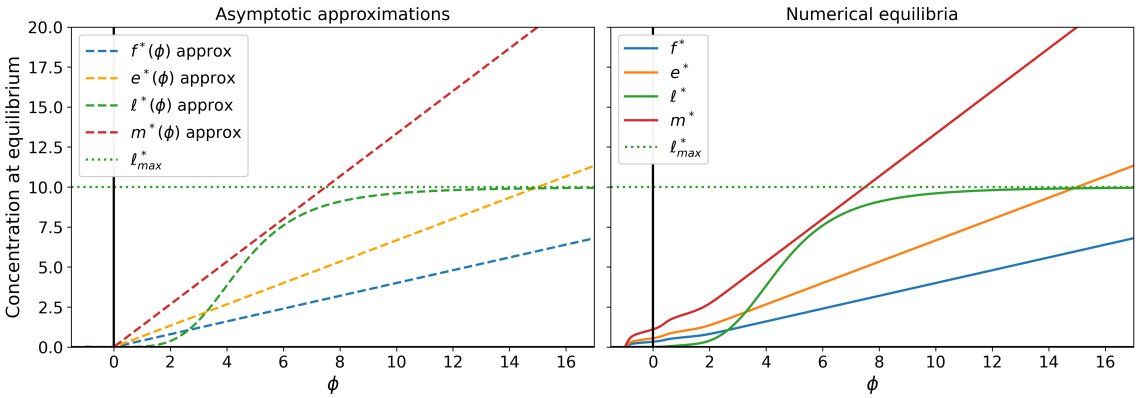


Figure 5: Plot showing comparison of equilibria and analytical approximations.

The approximations hold well for large ϕ values, with LH approaching its asymptote as expected. The difference between the numerical and analytical results for LH is only for small ϕ values where the approximation is not valid. We note that so far we have only considered constant dosages of FSH.

5 Optimisation of FSH Dosage

5.1 Natural Behaviour of the Model

If we simulate the system (Equations (4a) to (4d)) with constant zero dosage ($\phi = 0$), we see in Figure 6 that all variables converge to their equilibrium, as expected. What we note here is that with no additional FSH, the value of LH converges to a low value. Specifically, from Equation (8), when $\phi = 0$, we have that $e^* = e_{\min}$ and hence

$$\ell^* = \left[\frac{(e_{\min})^{n_6}}{(\kappa_6^+)^{n_6} + (e_{\min})^{n_6}}\right] \Big/ \left[\delta_L - \lambda_{L^-}\frac{(e_{\min})^{n_6}}{(\kappa_6^-)^{n_6} + (e_{\min})^{n_6}}\right]. \tag{20}$$

In Section 3.3, we said our model goes up to egg retrieval. We must collect the eggs before natural ovulation occurs as this is when the eggs would normally be released (see Appendix C for more details on ovulation). Hence, our model does not include the dynamics for natural ovulation. This is evident in Figure 6 as the value of LH converges to a low value when $\phi = 0$, indicating that ovulation has not occurred.

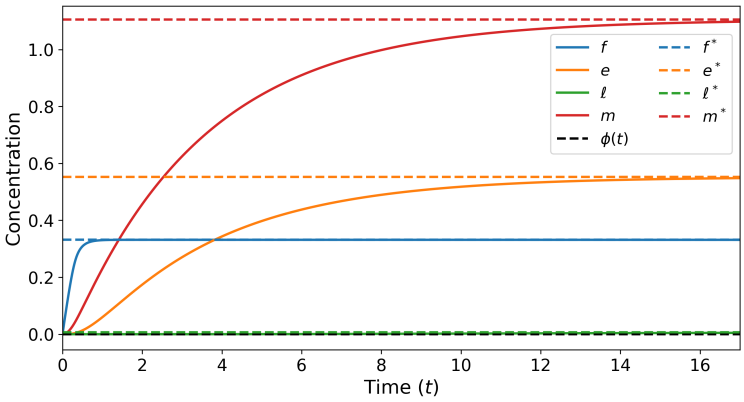


Figure 6: Plot showing the behaviour of all variables when $\phi = 0$ with initial conditions where each variable is set to zero.

5.2 Dosage Profiles

In theory, any $\phi(t) \geq 0$ is possible. However, to look at all possible dosage profiles would be impractical. Firstly, there will be a maximum safe dosage. Secondly, there will be practical limitations on how often and how precisely dosages can be administered. For example, it may not be possible to administer very small dosages at very frequent intervals. A dose must be absorbed and removed from the bloodstream, $\phi(t)$ and this is modelled by taking a sum of bell curves. Each centred at the maximum effect of the dose and with a maximum height ($\propto$ FSH dose) and a standard deviation. The latter would be a property of the drug and the specific patient. To keep things simple, we shall assume that all dosages have the same standard deviation.

Suppose we have N dosages administered within times $T = 0$ to T_F (when eggs are extracted) with standard deviation σ (the same for all) and τ_i, the mean[6], at times $\tau \in \mathbb{R}^N$ with heights (dosage strength) $d \in \mathbb{R}^N$. We express $\phi(t)$ exactly as

$$\phi(t) = \sum_{i=1}^{N} d_i \exp\left(-\frac{(t-\tau_i)^2}{2\sigma^2}\right). \quad (21)$$

For an example, see Figure 7.

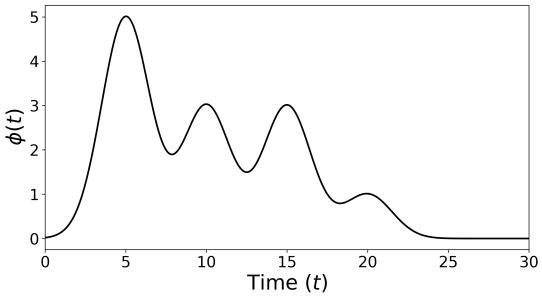


Figure 7: Example dosage profile: $N = 4$ with dosages at times $\tau^T = [5\ 10\ 15\ 20]$, strengths $d^T = [5\ 3\ 3\ 1]$, and $\sigma = 1.5$.

5.3 The Wearing-Off of FSH

The equilibrium for m is an important value to note. Suppose we choose a particular dosage profile $\phi(t)$ where it is positive in the interval $[0, T_1]$. Then also suppose that after some time $T_2 > T_1$ we see that $m(t) \approx m^*$. We may conclude that the FSH provided prior to T_2 has worn off. Specifically, we know that if $\tau_i + 3\sigma < T_F$, this dose has essentially worn off by time T_F. This is due to the number of mature follicles returning to when $\phi = 0$. This can clearly be seen in Figure 8 in that from $t = 40$ onwards the two schemes look identical. Hence, in our optimisation, we ignore dosage schemes where this occurs as it would be wasteful and costly to provide FSH that has no effect (assuming collection is after T_2).

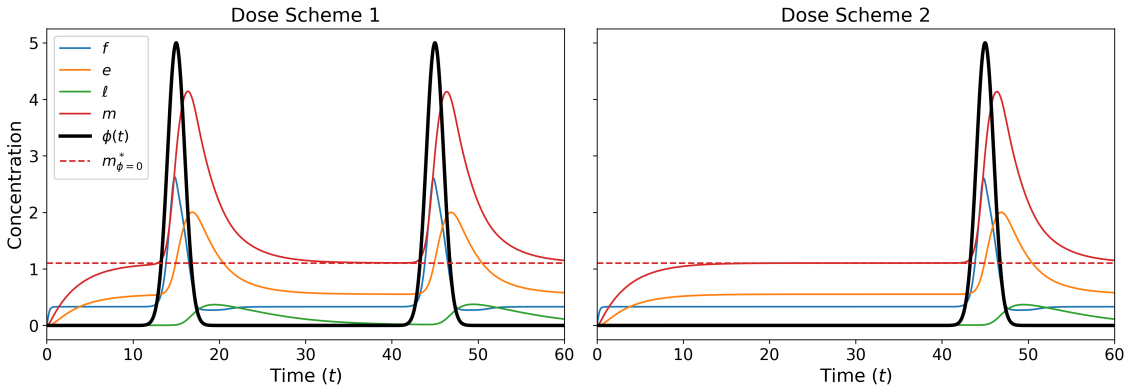


Figure 8: Plot showing how the effect of FSH dosage wears off over time.

[6]Technically, the bell curves have infinite support, implying a dosage at $t = -\infty$. However, for practical purposes, we consider them to be effectively zero before 3σ from the mean (this means that approximately 99.8% of the effect of that particular dose happens after the supposed injection time). As it is more convenient, we shall express these bell curves in terms of their mean τ_i. We also then have $3\sigma \leq \tau_i \leq T_F + 3\sigma$ with the lower bound imitating an injection taken at $t = 0$.

5.4 The Cost Function

When optimising the dosage profile in terms of its frequency and amount, we need to define a cost function. Otherwise we may recommend the maximum possible dosage at every time instant. An intuitive cost function, (C), would be the total volume of FSH administered over the treatment period (V) multiplied by its unitary cost. V can be calculated as the integral of the dosage profile[7],

$$\begin{aligned} V &= \int_{-\infty}^{\infty} \phi(t)\, dt \\ &= \int_{-\infty}^{\infty} \sum_{i=1}^{N} d_i \exp\left(-\frac{(t-\tau_i)^2}{2\sigma^2}\right) dt \\ &= \sigma\sqrt{2\pi} \sum_{i=1}^{N} d_i. \end{aligned} \tag{22}$$

We also note here that the volume of drug administered in each injection is given by $\sigma\sqrt{2\pi}d_i$ where we require $0 < d_i \leq d_{\max}$ (the maximum safe dosage). Hence, the cost function is proportional to the total volume of drug administered and could be written as: $C = \mu \sum_{i=1}^{N} d_i$, where $\mu = c\sigma\sqrt{2\pi}$, and c is the cost per unit volume.

5.5 Optimisation Problem Formulation

We now formulate the optimisation problem. We want to find the dosage profile $\phi(t)$ that maximises the number of mature follicles at time T_F, while keeping the cost low. This goal can be expressed mathematically as

$$\min_{\{d_i,\tau_i\}} \quad J = \underbrace{\mu \sum_{i=1}^{N} d_i}_{\text{drug cost}} - \underbrace{\lambda\, m(T_F)}_{\text{benefit}}. \tag{23}$$

Here, λ controls how much we value the number of mature follicles compared to the drug cost. A higher λ prioritises the number of mature follicles.

Equation (23) is subject to $f(t) < f_{\max}$ (this prevents us from injecting lots of small allowed d_i which would then become unsafe) and $\ell(t) < \ell_{\text{ov}}$ for all $t \in [0, T_F]$, where ℓ_{ov} is the threshold level of LH that would trigger ovulation. For some restriction on how accurate dosages can be, we shall enforce $d_i \in S_1 := \{a \times 10^b \mid a = \tilde{a}/10,\ \tilde{a} \in \mathbb{Z} \text{ and } 0 \leq \tilde{a} \leq 99,\ b \in \mathbb{Z}\}$. Where realistically, there is some minimum accuracy and $b_{\min} \leq b$ imposed by the lab equipment being used. Moreover, we can bound b above by $b_{\max} = \lfloor \log_{10}(d_{\max}) \rfloor$ to ensure we do not exceed the maximum safe dosage.

[7] We assume that if the drug is in use (inside the body) after T_F, we would still have to account for its cost. Hence, for simplicity, we shall integrate over $-\infty$ to ∞.

5.6 Reducing the Optimisation Problem

If we restrict τ_i to integers[8], we then have an integer optimisation problem. Then to allow greater control over the problem, for $0 \leq i \leq N-1$, impose $\tau_{i+1} - \tau_i \geq \Delta\tau_{\min}$ to ensure a minimum time between injections. Reasonably, we also impose $\tau_N \leq T_F$. From modelling solutions, we notice that for τ it is optimal to choose the latest possible times. This is because of the wearing-off discussed in Section 5.2. Hence, for a given number of dosages, N, and minimum time delay between injections, $\Delta\tau_{\min}$, assuming $\Delta\tau_{\min} \geq 1$, the optimal times will always be

$$\tau_i = T_F - (N-i)\Delta\tau_{\min}, \quad i = 1, 2, \ldots, N. \tag{24}$$

This is after further assuming that we want the peak effect of the dosage to have occurred before T_F. This is a reasonable assumption as we want the follicles to be affected by the majority of the dosage and not collected before it has a full effect.



Figure 9: Diagram showing optimal dosage timescale.

From Figure 9, we also get a condition relating the number of doses to the minimum time delay, $\Delta\tau_{\min}$. That is, given the dose wears off after 3σ from τ_i, we want $(N-1)\Delta\tau_{\min} < 3\sigma$. This guarantees that any dose we do take will have some effect at T_F. Given the context of the problem, we are more likely to want to control $\Delta\tau_{\min}$ to determine the number of doses rather than wanting a specific number of doses from the outset and determining a $\Delta\tau_{\min}$. Hence,

$$N^* = \left\lfloor \frac{3\sigma}{\Delta\tau_{\min}} \right\rfloor + 1. \tag{25}$$

This then determines τ, which is now given by

$$\tau_i = T_F - (N^* - i)\Delta\tau_{\min}, \quad i = 1, 2, \ldots, N^*. \tag{26}$$

This means we only need to optimise over the dosage strengths d, which scales down the complexity of the problem significantly.

[8] In theory, τ_i should be restricted to rational values, as this is the property being described. However, since numerical computation represents all quantities using finite-precision arithmetic, any implemented value of τ_i is rational, and thus no practical distinction arises between this and the real values we had before.

5.7 Problem Space Summary

To summarise, we have progressively constrained the optimisation problem to make it computationally feasible and practically relevant. The steps taken are as follows:

1. Started by searching for an optimal $\phi(t)$ over the infinite-dimensional space of piecewise continuous functions $\{\phi \in PC[0, T_F] \mid \forall\, t \in [0, T_F],\ 0 \leq \phi(t) \leq \phi_{\max}\}$.
2. Restricted $\phi(t)$ to be a sum of N bell curves with means τ and heights d, giving the space $\{N \in \mathbb{N}, d \in \mathbb{R}^N, \tau \in \mathbb{R}^N \mid 0 \leq d_i \leq d_{\max}, 0 \leq \tau_1 < \cdots < \tau_N \leq T_F\}$.
3. Restricted $d_i \in S_2 := \{a \times 10^b \mid a = \frac{\tilde{a}}{10},\ 0 \leq \tilde{a} \leq 99,\ b_{\min} \leq b \leq b_{\max},\ \tilde{a}, b \in \mathbb{Z}\}$ to represent the limitation on practical accuracy.
4. Enforced that τ_i must be integers to represent that dosages can only be administered at whole time intervals, not continuously.
5. Introduced a minimum time delay between dosages, $\Delta\tau_{\min}$, to ensure safety and practical control (e.g., preventing dosages too close together).
6. Determined that the optimal τ values would always occur at the latest possible times given N and $\Delta\tau_{\min}$, based on the wearing-off property of FSH.
7. Fixed N to be N^*, which is determined from the relationship $N^* = \left\lfloor \frac{3\sigma}{\Delta\tau_{\min}} \right\rfloor + 1$.
8. Arrived at the final optimisation space of $\{d \in S_2^{N^*}\}$.

Hence, the final size of the search space is

$$|S_2|^{N^*} = \left(100(\lfloor \log_{10}(d_{\max}) \rfloor - b_{\min} + 1)\right)^{\left\lfloor \frac{3\sigma}{\Delta\tau_{\min}} \right\rfloor + 1}, \tag{27}$$

which is still potentially very large. However, this is now a finite space that can be searched using integer programming techniques. An interesting observation is that the size of the search space grows exponentially with increasing σ. This is because a larger σ means that each dose has a longer effect, allowing for more doses to be administered within the time period when the drug has a resulting effect at T_F.

We further note that S_2 still leads to profiles (ϕ) that are not allowed, as the LH levels may at some point be high enough to trigger premature ovulation or E2 may exceed safe limits. These constraints must be enforced during optimisation, but determining if they are violated requires solving the system each time.

Another useful observation is that if we were to compute all possible dosage profiles or a reasonable subset, we could store the results. From this we could tweak certain parameters such as λ, μ, $f_{\max}$ or ℓ_{ov} without needing to re-solve any system. This is because these parameters only affect the cost function and constraints, not the system dynamics.

6 An Optimal Solution Example

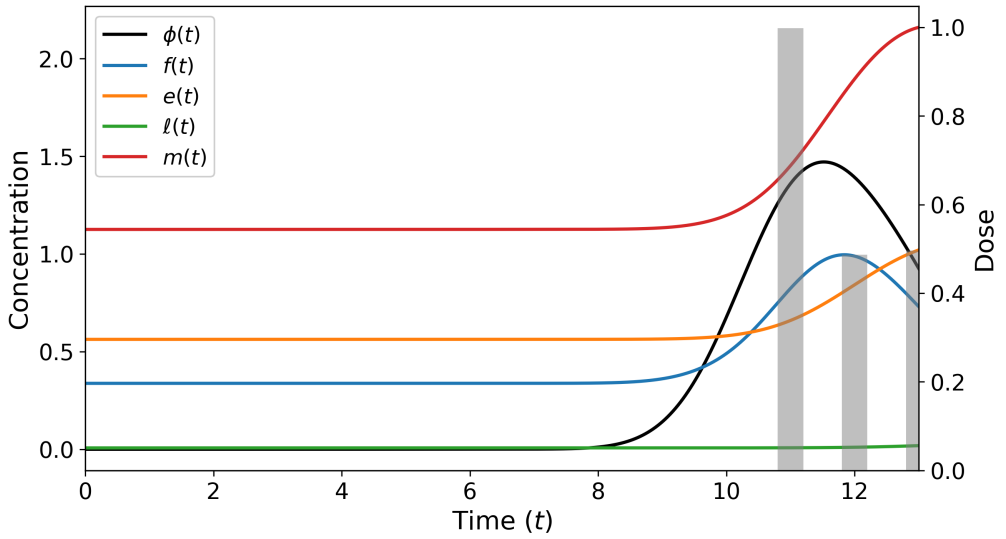


Figure 10: Plot showing optimisation of FSH dosage profile.

We see in Figure 10 an optimal dosage profile for a particular weighting, $\lambda = 5$, and a supposed cost, $\mu = 2$. We have set the initial conditions for f, e, ℓ and m to be the equilibria calculated in Equations (16) to (19) and parameters from Figure 4 given in Appendix B. In the optimising process, we had $N^* = 11$ assuming $\sigma = 1 = \Delta\tau_{\min}$. This equates to assuming the drug will be in the system for 6 days[9] and that we could have one dosage taken per day. We note that although in our problem construction we had restrictions on both f and ℓ (specifically we chose $f_{\max} = 1$ and $\ell_{\text{ov}} = 0.1$), in practice only the former has been hit and constrained this solution. But this could very easily change depending on the parameters.

This particular solution suggests the optimal dosage schedule would be to inject 1 unit of FSH on day 11 and 0.5 on days 12 and 13. The dosage is reduced to ensure that f stays below the safe limit. This results in $m(T_F) = 2.17$ $(3\ s.f.)$ mature follicles at a total cost of $C = 2.5\mu$. Interestingly, we get the same solution for d if we remove the assumption that τ_i will be at the latest possible times. This further validates our hypothesis about the optimal τ.

From this example, we see that the optimisation problem set out is able to solve the simplified problem for reasonable dosage profiles that balance cost and benefit. However, this is only a crude result and further work is needed to explore the parameter space (of which there are many) and validate the model against real-world data.

[9] As we are dealing with a non-dimensionalised system, we do not actually have any units, however it is convenient to call the unit in t a day.

7 Conclusion

In this work, we have developed a simple model of the ovarian follicle dynamics under the influence of FSH. We then justified its feasibility or required particular conditions to ensure this in a physiological context. We used Hill functions to model the hormonal interactions and a system of ordinary differential equations to describe the dynamics.

Analysing the equilibria of the system under constant FSH dosages, we found a curious phenomenon; the LH equilibria were bounded above by $\ell_{\max}$. This shows that for this particular model, no matter how much FSH is administered, LH will never exceed this value. This may be helpful in parameterising the model with real-world values because we know that $\ell_{\max}$ should be above the ovulation threshold, which will be a known quantity. Otherwise, the model could never exhibit premature ovulation, which it should do as this is an issue faced in the real-world.

We then formulated an optimisation problem to determine optimal FSH dosage profiles assuming a bell-curve for the dosage profile. This problem was trying to solve the issue of maximising the number of mature follicles at egg retrieval time whilst minimising the amount of the drug used. We simplified the problem by putting realistic bounds on when we could administer the drug and how accurately the dose could be measured. These assumptions moved the problem to an integer programming problem. This could then be solved to find optimal dosage profiles. The hypothesis we made about the τ_i values occurring at the latest possible times was also verified through numerical experimentation.

8 Future Perspectives

There are many directions this work could be taken in. This could include obtaining real-world values for the parameters in the model. The issue with this is that the model is currently far too simplistic to contain the wealth of information that would be needed for this to be used in practice. We would need to include other hormones such as GnRH and Inhibin, as well as enter details about the woman. For example, age and weight have appeared as important factors in the referenced papers. Moreover, the range of values and nonuniformity of their spatial distribution, along with a host of other medical and biological factors would need to be considered to get an accurate picture to start modelling from.

An alternative direction would be to consider a more general dosage profile. So not restricting to a linear sum of bell curves, but instead considering how there may be a limit to how receptive the body is to FSH after a certain dosage, e.g. a saturation effect rather than directly incrementing the FSH level in the bloodstream.

9 References

[1] M. C. Chang, "Fertilization of rabbit ova in vitro," *Nature*, vol. 184, no. 4684, pp. 466–467, 1959.

[2] C. Feltham and I. Horton, *The SAGE handbook of counselling and psychotherapy*. SAGE, 2006, ISBN: 1-4129-0274-6.

[3] Guy's and St Thomas' NHS Foundation Trust. "Risks of IVF," Accessed: Dec. 7, 2025. [Online]. Available: https://www.guysandstthomas.nhs.uk/health-information/ivf-treatment/risks-ivf.

[4] Human Fertilisation and Embryology Authority. "Decisions to make about your embryos," Accessed: Dec. 7, 2025. [Online]. Available: https://www.hfea.gov.uk/treatments/explore-all-treatments/decisions-to-make-about-your-embryos/.

[5] University Hospitals Coventry & Warwickshire NHS Trust. "Price list 2025 (gen-pi-000211v52)." PDF document listing clinical service prices, Accessed: Feb. 16, 2025. [Online]. Available: https://www.uhcw.nhs.uk/download/clientfiles/files/Price%20List%202025%20(GEN-PI-000211V52).pdf.

[6] C. González Arboleya and D. Sosa. "Ovulation induction in IVF: Medical stimulation control." Includes ultrasound image of ovarian follicles during controlled ovarian stimulation, Accessed: Dec. 16, 2025. [Online]. Available: https://www.invitra.com/en/ovulation-induction-in-ivf/stimulation-medical-control/.

[7] I. Reinecke and P. Deuflhard, "A complex mathematical model of the human menstrual cycle," *Journal of Theoretical Biology*, vol. 247, no. 2, pp. 303–330, 2007.

[8] C. A. Christian, C. Glidewell-Kenney, J. L. Jameson, and S. M. Moenter, "Classical estrogen receptor α signaling mediates negative and positive feedback on gonadotropin-releasing hormone neuron firing," *Endocrinology*, vol. 149, no. 11, pp. 5328–5334, 2008.

[9] W. Vegetti and F. Alagna, "FSH and folliculogenesis: From physiology to ovarian stimulation," *Reproductive Biomedicine Online*, vol. 12, no. 6, pp. 684–694, 2006.

[10] L. A. Harris and J. F. Selgrade, "Modeling endocrine regulation of the menstrual cycle using delay differential equations," *Mathematical Biosciences*, vol. 257, pp. 11–22, 2014.

[11] K. L. Herbst, "Gonadotropin-releasing hormone antagonists," *Current Opinion in Pharmacology*, vol. 3, no. 6, pp. 660–666, 2003.

[12] R. Lopez, *Ovarian hormones throughout the menstrual cycle*, BioRender template, 2025. Accessed: Dec. 10, 2025. [Online]. Available: https://app.biorender.com/profile/template/details/t-642310511f9d75406597259a-ovarian-hormones-throughout-the-menstrual-cycle.

Appendix

A Glossary

Acronym	Definition
COS	controlled ovarian stimulation
E2	estradiol
FSH	follicle stimulating hormone
GnRH	gonadotropin-releasing hormone
HFEA	Human Fertilisation and Embryology Authority
ICSI	intracytoplasmic sperm injection
IVF	in vitro fertilization
LH	luteinizing hormone
ODE	ordinary differential equation
OHSS	ovarian hyperstimulation syndrome
P4	progesterone

B List of Parameters

The list of parameters first used in Figure 4 and throughout the work is given in Table 1 below.

λ parameters		κ parameters		δ parameters		n parameters	
Parameter	Value	Parameter	Value	Parameter	Value	Parameter	Value
λ_F	1.5	κ_2	1	δ_E	2	n_2	11
λ_L	1	κ_3	0.3	δ_L	1.1	n_3	7
		κ_6^+	3	δ_M	0.3	n_6	4
		κ_6^-	0.3				

Table 1: Grouped model parameter values used in simulations.

C Background on the Menstrual Cycle

The menstrual cycle is a complex sequence of events dependent on hormones that regulate ovulation and prepare the body for potential pregnancies. The key hormones are FSH, LH produced by the pituitary gland, E2, and progesterone (P4) produced by the ovaries. The cycle can be divided into four sections: menstruation, the follicular phase, ovulation, and the luteal phase.

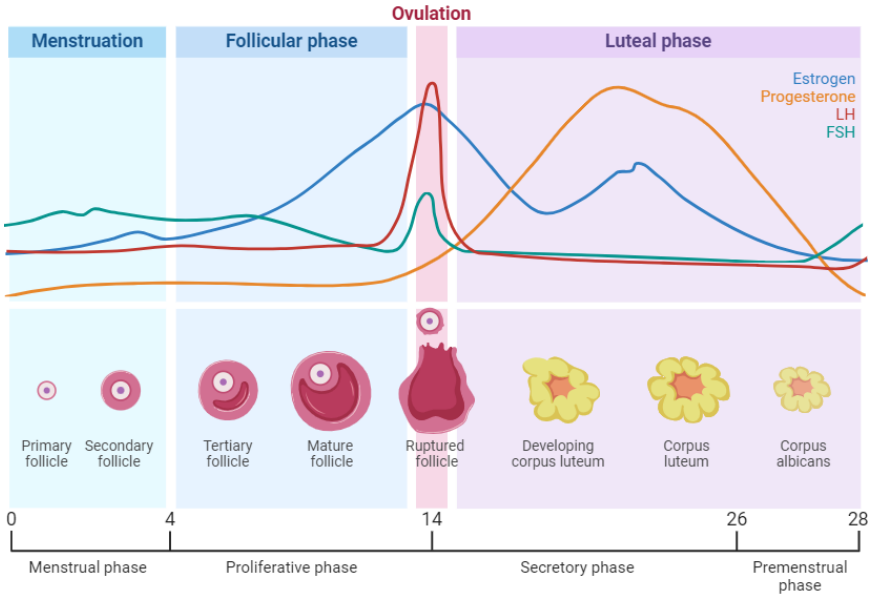


Figure 11: The menstrual cycle phases and hormone levels [12].

At the beginning of the cycle, the pituitary gland in the brain releases the hormone FSH. This is carried in the bloodstream and picked up on the surface of the cells of the ovaries. Inside the ovaries are hundreds of thousands of follicles. These are small sack-like structures that contain 'ova' — the immature eggs. In response to the FSH, two things happen. First, some follicles start to grow and mature. Second, the ovaries start to make and release E2. The E2 travels in the bloodstream to the uterus, where it causes the lining to thicken in preparation for a possible pregnancy later in the cycle.

The rise in E2 also has an effect on the brain. It causes the pituitary gland to reduce the amount of FSH it is releasing. This is a negative feedback loop that prevents too many follicles from maturing at once. The E2 also causes the pituitary gland to release LH. The sudden rise in LH causes the most mature follicle to release its egg — this is called ovulation. The egg then travels along the Fallopian tubes towards the uterus.

After ovulation, the follicle that released the egg forms a structure called the corpus luteum. This structure releases P4 into the bloodstream. The P4 has two main effects. First, inhibits the release of LH and continues to inhibit FSH production. It also keeps the uterus lining thick and ready for a fertilised egg to implant.

If the egg is fertilised, the egg embeds itself in the uterus lining. The ovary continues making P4, and this then triggers all the changes that are part of pregnancy. If the egg is not fertilised, the corpus luteum breaks down, which means it no longer produces P4. This also causes the levels of E2 in the blood to fall. The drop in these hormones signals to the uterus that there is no pregnancy, so the uterus sheds the lining. The drop in P4 and E2 also signals to the brain to start releasing FSH again, and the cycle starts over. This is summarised in Figure 12.

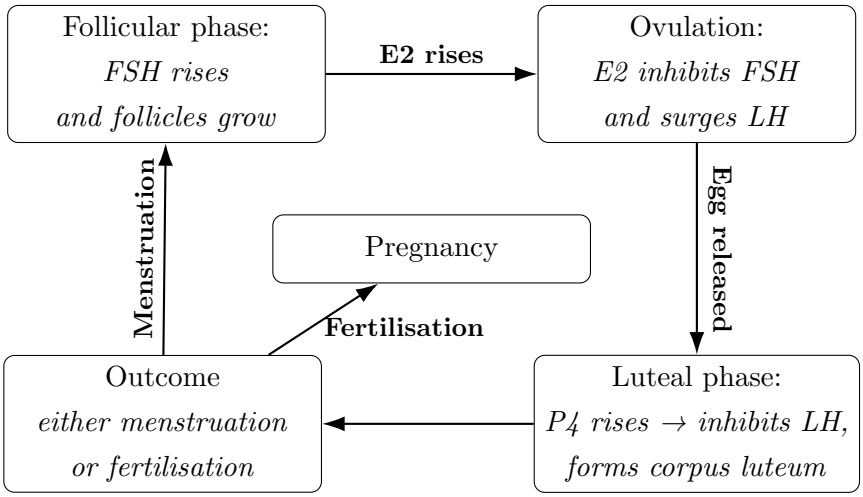


Figure 12: Schematic of menstrual cycle stages.

D Full LH Model from Selgrade and Harris

The full LH model from Selgrade and Harris [10] is given by the following system:

$$\frac{d}{dt}RP_{LH} = syn_{LH}(E_2, P_4) - rel_{LH}(E_2, P_4, RP_{LH}), \tag{28a}$$

$$\frac{\mathrm{d}}{\mathrm{d}t}LH = \frac{1}{v}rel_{LH}(E_2, P_4), RP_{LH} - clear_{LH}(LH). \tag{28b}$$

where

- RP_{LH} is the reserve pool of LH,
- LH is the concentration of LH in the bloodstream,
- v is the volume of distribution,
- syn_{LH} is the synthesis rate of LH,
- rel_{LH} is the release rate of LH from the reserve pool to the bloodstream,
- $clear_{LH}$ is the clearance rate of LH from the bloodstream.

E Full Non-dimensionalisation of the Model

To non-dimensionalise the model, we introduce the following dimensionless variables and parameters:

$$\tau = T\,t, \quad F = F_0\,f, \quad E = E_0\,e, \quad L = L_0\,\ell, \quad M = M_0\,m,$$

where T, F_0, E_0, L_0, and M_0 are characteristic scales for FSH, E2, LH, and mature follicles respectively. Then, if we start by substituting the Hill functions into the dimensional system, we have

$$\frac{\mathrm{d}F}{\mathrm{d}\tau} = -\gamma_F F - \beta_F F \frac{E^{n_2}}{K_2^{n_2} + E^{n_2}} + \alpha\left(1 - \frac{F^{n_3}}{K_3^{n_3} + F^{n_3}}\right) + u, \tag{29a}$$

$$\frac{\mathrm{d}E}{\mathrm{d}\tau} = -\gamma_E E + \beta_E M, \tag{29b}$$

$$\frac{\mathrm{d}L}{\mathrm{d}\tau} = -\gamma_L L + \beta_{L^+}\frac{E^{n_6}}{(K_6^+)^{n_6} + E^{n_6}} - \beta_{L^-} L\left(1 - \frac{E^{n_6}}{(K_6^-)^{n_6} + E^{n_6}}\right), \tag{29c}$$

$$\frac{\mathrm{d}M}{\mathrm{d}\tau} = -\gamma_M M + \beta_M F. \tag{29d}$$

Then, substituting in the non-dimensional variables gives

$$\frac{F_0}{T}\frac{\mathrm{d}f}{\mathrm{d}t} = -\gamma_F F_0 f - \frac{\beta_F (F_0 f)\,(E_0 e)^{n_2}}{K_2^{n_2} + (E_0 e)^{n_2}} + \alpha\left(1 - \frac{(F_0 f)^{n_3}}{K_3^{n_3} + (F_0 f)^{n_3}}\right) + u(Tt), \tag{30a}$$

$$\frac{E_0}{T}\frac{\mathrm{d}e}{\mathrm{d}t} = -\gamma_E E_0 e + \beta_E M_0 m, \tag{30b}$$

$$\frac{L_0}{T}\frac{\mathrm{d}\ell}{\mathrm{d}t} = -\gamma_L L_0 \ell + \frac{\beta_{L^+}\,(E_0 e)^{n_6}}{(K_6^+)^{n_6} + (E_0 e)^{n_6}} - \beta_{L^-} L_0 \ell\left(1 - \frac{(E_0 e)^{n_6}}{(K_6^-)^{n_6} + (E_0 e)^{n_6}}\right), \tag{30c}$$

$$\frac{M_0}{T}\frac{\mathrm{d}m}{\mathrm{d}t} = -\gamma_M M_0 m + \beta_M F_0 f. \tag{30d}$$

Rearranging gives

$$\frac{\mathrm{d}f}{\mathrm{d}t} = -\gamma_F T f - \beta_F T \frac{f e^{n_2}}{\left(\frac{K_2}{E_0}\right)^{n_2} + e^{n_2}} + \frac{\alpha T}{F_0}\left(1 - \frac{f^{n_3}}{\left(\frac{K_3}{F_0}\right)^{n_3} + f^{n_3}}\right) + \frac{T}{F_0}u(Tt), \tag{31a}$$

$$\frac{\mathrm{d}e}{\mathrm{d}t} = -\gamma_E T e + \frac{\beta_E M_0 T}{E_0} m, \tag{31b}$$

$$\frac{\mathrm{d}\ell}{\mathrm{d}t} = -\left(\gamma_L T + \beta_{L^-} T\right)\ell + \frac{\beta_{L^+} T}{L_0}\frac{e^{n_6}}{\left(\frac{K_6^+}{E_0}\right)^{n_6} + e^{n_6}} + \beta_{L^-} T \frac{\ell e^{n_6}}{\left(\frac{K_6^-}{E_0}\right)^{n_6} + e^{n_6}}, \tag{31c}$$

$$\frac{\mathrm{d}m}{\mathrm{d}t} = -\gamma_M T m + \frac{\beta_M F_0 T}{M_0} f. \tag{31d}$$

If we choose $T = \frac{1}{\gamma_F}$, $F_0 = \frac{\alpha}{\gamma_F}$, $E_0 = \frac{\alpha\beta_E\beta_M}{\gamma_F^3}$, $L_0 = \frac{\beta_{L^+}}{\gamma_F}$, $M_0 = \frac{\alpha\beta_M}{\gamma_F^2}$, then

$$\frac{\mathrm{d}f}{\mathrm{d}t} = -f - \lambda_F \frac{f e^{n_2}}{\kappa_2^{n_2} + e^{n_2}} + \left(1 - \frac{f^{n_3}}{\kappa_3^{n_3} + f^{n_3}}\right) + \phi(t), \tag{32a}$$

$$\frac{\mathrm{d}e}{\mathrm{d}t} = -\delta_E e + m, \tag{32b}$$

$$\frac{\mathrm{d}\ell}{\mathrm{d}t} = -\delta_L \ell + \frac{e^{n_6}}{(\kappa_6)^{+n_6} + e^{n_6}} + \lambda_{L^-} \frac{\ell e^{n_6}}{(\kappa_6)^{-n_6} + e^{n_6}}, \tag{32c}$$

$$\frac{\mathrm{d}m}{\mathrm{d}t} = -\delta_M m + f. \tag{32d}$$

Here

- $\delta_E = \frac{\gamma_E}{\gamma_F}$, $\delta_L = \frac{\gamma_L + \beta_{L^-}}{\gamma_F}$, $\delta_M = \frac{\gamma_M}{\gamma_F}$ are the dimensionless clearance/decay rates,
- $\kappa_2 = \frac{K_2\gamma_F^3}{\alpha\beta_E\beta_M}$, $\kappa_3 = \frac{K_3\gamma_F}{\alpha}$, $\kappa_6^+ = \frac{K_6^+\gamma_F^3}{\alpha\beta_E\beta_M}$, $\kappa_6^- = \frac{K_6^-\gamma_F^3}{\alpha\beta_E\beta_M}$ are the dimensionless half-saturation constants,
- $\lambda_F = \frac{\beta_F}{\gamma_F}$, $\lambda_{L^-} = \frac{\beta_{L^-}}{\gamma_F}$ are dimensionless production rate parameters,
- $\phi(t) = \frac{1}{\alpha} u\left(\frac{t}{\gamma_F}\right)$ is the dimensionless FSH dosage.